To Be or Not to Be a Molecular Ion: The Role of Solvent in Photoionization of Arginine

Alexandre Barrozo[a]*, Bo Xu[b]*, Anastasia O. Gunina[a], Michael Jacobs[b], Kevin Wilson[b], Oleg Kostko[b], Musahid Ahmed[b], Anna I. Krylov[a,c]

[a]Department of Chemistry, University of Southern California, Los Angeles, California 90089-0482

[b]Chemical Sciences Division, Lawrence Berkeley National Laboratory, Berkeley, CA 94720

[c]The Hamburg Centre for Ultrafast Imaging, Luruper Chaussee 149, 22671 Hamburg, Germany

*These authors contributed equally

Application of photoionization mass spectroscopy, a technique capable of assessing protonation states in complex molecules in the gas phase, is challenging for arginine due to its fragility. We report photoionization efficiencies in the valence region of aqueous aerosol particles produced from arginine solutions at various pH and vaporization conditions. By using *ab initio* calculations, we investigate the stability of different conformers. Our results show that neutral arginine fragments upon ionization in the gas phase but solvation stabilizes the molecular ion, resulting in different photoionization dynamics. We also report the valence-band photoelectron spectra of the aerosol solutions obtained at different pH.

By using proteins and DNA as templates for molecular electronics and sensors, exquisite chemical sensing technologies can now monitor processes relevant to human health and environmental remediation. This has been accomplished thanks to advances in techniques capable of probing physical and chemical properties of these molecules. For instance, the advent of soft ionization techniques started a revolution in biological mass spectrometry. Yet, characterization of amino acids in the gas phase is not trivial. In fact, there has not been an experimental determination of the ionization energy of one amino acid: arginine. Arginine has multiple protonation sites that endow it with the ability to form multiple hydrogen-bond patterns, which is important for structural purposes within proteins and for its other biological roles, such as sensing membrane potentials[1,2]. Arginine was also shown to be essential for formation of prenucleation clusters used as an alternative crystallization pathway[3]. Its exact protonation state in proteins, where it is found almost almost exclusively

in the cationic state, was a subject of debate[4]. Experimental characterization of possible protonation states of arginine by using techniques such as photoionization mass spectroscopy is challenging because transporting these non-volatile and very fragile molecules to the gas phase leads to extensive fragmentation. The electronic properties of gas-phase arginine were widely investigated. One question was the existence and stability of zwitterionic forms[5–14]. To form a stable zwitterion, the coulombic energy gained from the interaction of oppositely charged groups must exceed the difference in basicity between the protonated base and the deprotonated acid.

Setting the record among all natural amino acids, arginine has over a hundred isomers. Even at low temperatures, several isomers have considerable equilibrium populations. At room temperature, at least eight isomers are present[11]; their structures and labels are shown in Fig. S3 in SI. The large number of isomers arises due to the long and flexible side chain with the guanidine group, which can form various hydrogen bonds. In gas phase, conformers of canonical and tautomeric types (labeled c and t in Fig. 1) are the most abundant. The existence of a zwitterionic form (z) in the gas phase has been debated[8], but *ab initio* calculations showed[11] that it is thermally accessible, despite its higher energy. According to the same study, among various protonated arginine forms, pg is prevalent in the gas phase. In aqueous solutions, however, core ionization experiments identified p as the prevalent form at neutral and moderately basic conditions[15]. Zwitterionic forms become dominant only at very basic pH[15].

Over a decade ago, we developed a method of introducing fragile and labile molecules to the gas phase[16,17] without fragmenting them. The technique entails impacting intense focused particle beams, generated by aerosol methods and aerodynamic focusing, on a thermal heater. This approach produces intact amino acids. Arginine and histidine are notorious for fragmentation in mass spectrometers. By using the aerosol method, we were able to generate unfragmented histidine and to determine its ionization energy for the first time[17]. Recently, we interrogated the protonation state of arginine as a function of solution pH with X-ray photoelectron spectroscopy and reported[15] a surprising result: the guanidinium group remains protonated in a very basic solution (pH 13). This led us to posit that it is the nature of solvation of arginine that might dictate the fragmentation behavior that we observe upon valence photoionization.

In this Letter, we present the results of extensive experimental and theoretical in-

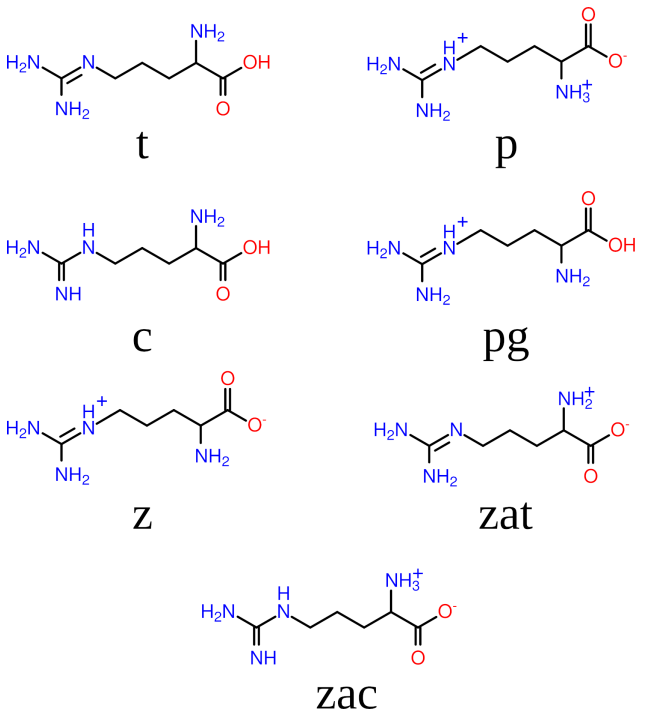

FIG. 1: Different forms of neutral (*t*, *c*, *z*, *zat*, *zac*) and protonated (*p*, *pg*) arginine. Left panel shows gas-phase forms.

vestigation aiming to determine the ionization energy of arginine and to quantify how solvation affects it. We report photoionization mass-spectrometry results for gas-phase arginine extracted from aerosols under various pH conditions. Specifically, we determined appearance energies for the parent ion and various fragments. This is the first experimental report on the IE of gas-phase arginine. We then applied valence-band photoelectron spectroscopy to the aerosol beam of aqueous arginine under similar pH conditions. To understand how valence-level photoionization affects arginine in the gas and solvated phases, we carried out *ab initio* calculations. The calculations reveal extreme fragility of the ionized arginine in the gas phase, thus explaining the low yield of the parent ion in the mass-spectra, and a strong effect of the solvent on the ionization-induced dynamics. The combined experimental and theoretical results provide a new detailed picture of the photoionization of this most basic amino acid.

Aqueous aerosols with a mean diameter of 170 nm were generated by atomizing arginine-water solution (0.1 mol/L) at different pH conditions. The aerosol was tightly focused into a beam after passing through a set of aerodynamic lenses. In the mass-spectrometric study,

the focused aerosols were impacted on a thermal heater located within the time-of-fight (TOF) optics of a VUV mass spectrometer[17]. Gas-phase arginine molecules produced by vaporization of the particles were subsequently photoionized by tunable VUV light. The generated ions were analyzed by a reflectron TOF mass spectrometer. The undulator of the Chemical Dynamics Beamline (9.0.2) at the LBNL Advanced Light Source was continuously scanned, and mass spectra were collected in 0.1 eV steps. After correcting for photon flux, the photoionization efficiency curves were extracted for each mass. In the photoelectron spectroscopic study, photoemission from a focused aqueous aerosol beam was measured using a velocity map imaging spectrometer[18]. Additional details are given in SI.

We computed vertical ionization energies (VIE) of the most abundant isomers using the EOM-IP-CCSD/MP2 methods[19,20]. To understand structural relaxation induced by ionization, we performed geometry optimization of ionized arginine molecules and *ab initio* molecular dynamics (AIMD) calculations using density functional theory. To model ionization in aqueous solution, we carried out calculations with implicit (CPCM) and explicit solvent models. In the latter calculations, the solvent molecules were described either by point charges (QM/MM protocol) or by effective fragment potentials (EFP), here referred to as the QM/EFP protocol[21,22]. In the explicit solvent calculations, we performed configuration sampling of arginine solvated in water by using equilibrium MD simulations. All electronic structure calculations were carried out with the Q-Chem package[23] and MD simulations were performed using GROMACS[24]. The computational details are provided in the SI.

Fig. 2 shows mass spectra of gas-phase arginine obtained from solutions at pH of 1, 7, and 13. The spectra demonstrate very little intensity of arginine cation ($\frac{m}{z} = 174$) at pH 1, which further decreases at pH 7, and finally disappears at pH 13. In contrast, large amounts of fragment ions are generated at all three pH conditions. The low signal of the arginine cations and strong intensity of the fragment ions suggest that the arginine cations are not stable and can easily dissociate. The photoionization curves of arginine and major fragment species are shown in Fig. 2d. Using a non-linear least square fitting technique, we derived the appearance energy (AE) of 8.05±0.1 eV for the arginine cation (Table S1 in SI). Note that the AE of fragment ions with $\frac{m}{z}$ equal to 157 (AE = 8.18 eV, corresponding to the loss of NH_3) and 156 (AE = 8.10 eV, due to the loss of H_2O) are very close to that of arginine cation, suggesting that ionized arginine likely undergoes rapid fragmentation.

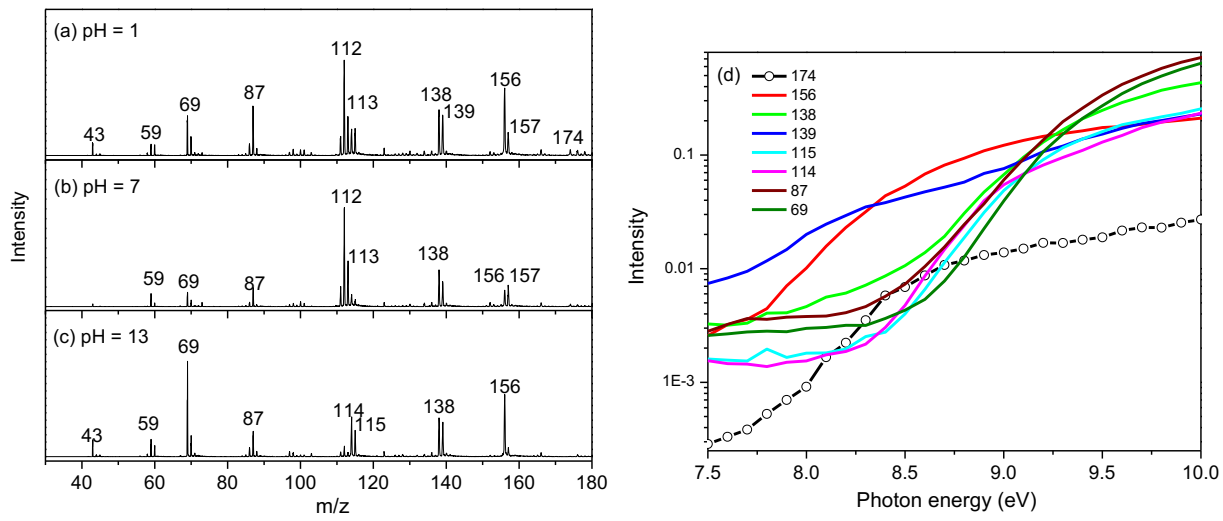

FIG. 2: Panels (a)-(c): mass spectra of gas-phase arginine generated from solutions at pH of 1, 7, and 13, measured at 9 eV. Panel (d): photoionization efficiency curves of arginine and major fragments at pH 1. Note the log scale in the y axis to highlight the paucity of the parent ion signal.

To model gas-phase ionization of arginine, we computed VIEs for eight of the lowest-lying conformers[11]: five of the tautomeric type, one canonical, and two zwitterionic conformers (see Fig. S3). The first VIE of each structure and the respective Dyson orbitals[25] are shown in Fig. S4. The VIEs range between 8.0-9.0 eV for different conformers. The corresponding Dyson orbitals are rather delocalized. They show large amplitudes on the guanidine group in the canonical and tautomeric conformers. Structures $t4$ and $t5$ also show significant density on the oxygens. In contrast, the two zwitterionic structures have large amplitudes on the carboxylate and amine groups. For all structures, multiple ionized states can be accessed within 2 eV from the lowest VIE. For canonical and tautomeric structures, we computed nine ionized states for each structure and for zwitterionic structures we computed five ionized states. The resulting stick spectra are shown in Fig. S5 in SI. We note that all states correspond to Koopmans-like transitions (except for having dominant contributions from HOMO-2 and HOMO-1 in states 2 and 3, respectively, in both zwitterions, $z7$ and $z8$), with the norms of Dyson orbitals of 0.94-0.95.

The geometry optimization of the ionized species (starting from the Franck-Condon structures) revealed that conformers $t4$, $t5$, and $z7$ undergo barierrless dissociation, producing neutral CO_2 and amine cations. The dissociation is highly exothermic: about 2.2 eV for the tautomeric conformers and 1.6 eV for the zwitterion. For other isomers, we were able to

identify stable structures. We observed substantial energy relaxation (0.7-1.1 eV), as well as significant changes in the optimized structures of non-dissociating ionized conformers relative to the respective neutral structures. The lowest adiabatic IE (AIE) is 7.4 eV ($t1$, $t2$, and $z8$ structures), followed by 7.5 eV for $t6$, and 7.7 eV for the canonical structure. Dyson orbitals and AIEs are shown in Fig. S4 and S5.

Large energy and geometry relaxation suggests unfavorable Franck-Condon factors for the 0–0 transition. Even more important is the fragility of the ionized arginine molecules: since several isomers undergo barierrless fragmentation in the Franck-Condon region, one can expect that other structures might have sufficient excess energy to overcome small barriers separating them from the dissociative region of the potential energy surface. To test this assumption and to identify most likely fragmentation channels, we carried out constant-energy AIMD simulations for the following isomers: $t1$ (similar to $t2$ and $t6$), $c3$, $t4$ (similar to $t5$, both dissociate upon geometry optimization), and $z8$ (similar to $z7$, but does not dissociate upon geometry optimization). We used three different initial conditions: corresponding to: the excess energy of 1 eV (the estimated maximal excess energy imparted by the ionizing photons), 0.1 eV, and 400 K (temperature of the heater). The trajectories show that ionized arginine undergoes rapid dissociation on less than 50 fs timescale. At 400 K, conformers $t1$ and $t4$ exhibit proton transfer to guanidine forming zwitterionic structures, followed by CO_2 elimination. Zwitterionic form $z8$ also dissociates promptly. In all cases, the resulting cations remained stable throughout the rest of the simulation, *i.e.*, for about 10 ps. AIMD simulations of the neutral molecules with the initial velocities corresponding to 400 K thermal distribution did not lead to dissociation. Thus, the calculations show that while neutral gas-phase arginine is stable under the experimental conditions, ionization leads to rapid and extensive fragmentation. In combination with the unfavorable Franck-Condon factors, this gives rise to a very small yield of the parent cation and explains the low signal. We note that the experimental onset of 8.05±0.1 eV is the closest to the computed AIE of the canonical isomer (∼7.7 eV) that did not dissociate. More abundant tautomeric forms and zwitterionic isomer have lower AIE of 7.5 eV (computed), and undergo dissociation in the AIMD simulations already at 400 K. Thus, we do not expect these forms to contribute to the $\frac{m}{z}$=174 photoionization signal. Consequently, we assign the experimental photoionization onset of 8.05±0.1 eV to the ionization of the canonical isomer.

Electrostatic and polarization interactions strongly affect conformers' distribution and

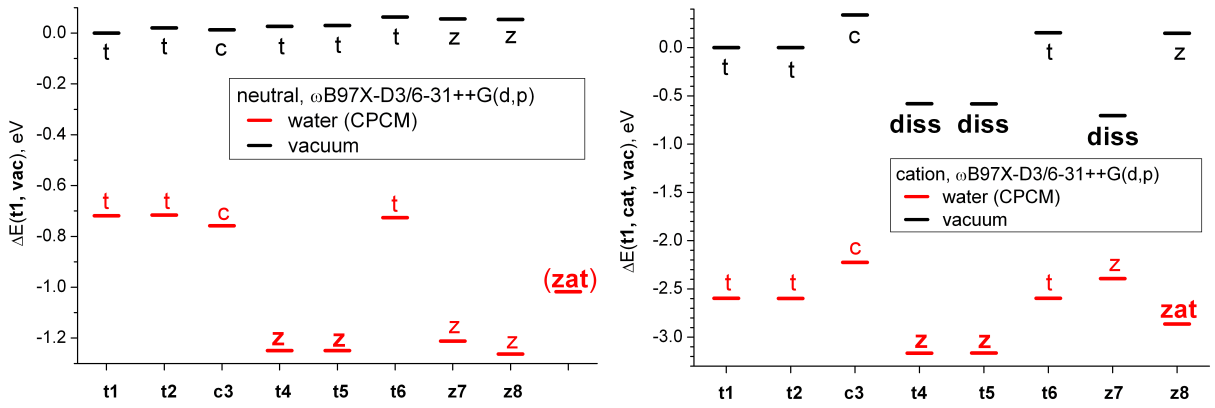

FIG. 3: Relative energies of the neutral isomers of arginine (left) and their respective ionized forms (right). Labels correspond to the types of structures shown in Fig. 1. Labels on the x-axis correspond to the neutral gas-phase isomers (see Fig. S3 in SI). The energies of the neutral species are given relative to the energy of the gas-phase $t1$ structure. The energies of the the ionized species are given relative to the energy of the gas-phase $t1$ cation.

the IEs of biological molecules in condensed phase[26–28] and arginine is no exception. Fig. 3 shows relative energies of the optimized structures of the neutral and ionized isomers of arginine in gas phase and solution (solvent effects are described by CPCM). Their structures and labels are shown in Fig. S3, with the respective energies collected in Table S2. The left panel shows relative energies of the dominant conformers of neutral arginine. The solvent has a large effect on the relative energies of the isomers, strongly stabilizing the zwitterionic isomers, with a difference of 0.3–0.5 eV relative to the canonical and tautomeric forms. In the gas phase, the differences in energies between the 8 structures are less than 0.1 eV. The right panel shows relative energies of the ionized species. The energy spread for the ionized gas-phase structures is larger than that for the neutrals, *e.g.*, stable gas-phase cationic structures can differ by as much as ∼0.4 eV. Solvation energies for the neutral forms range between 0.7–1.3 eV, whereas for the ionized structures, the solvation energies are 2–3 eV. As in the case of neutral structures, the lowest-energy ionized structures correspond to zwitterionic forms. Among solvated ionized structures, a new type of structure appears, labeled *zat*. In contrast to the gas phase, optimization of the ionized structures in CPCM results in stable structures. Thus, the calculations reveal strong stabilizing effect of the solvent on the ionized arginine, as illustrated in Fig. 3.

To study the effect of the solvent on the ionization energy of arginine, we obtained photoelectron spectra of aqueous arginine nanoparticles generated from solutions at various

pHs using 12 eV and 15 eV photons. Fig. 4a shows the spectra obtained at 12 eV; the spectra obtained with 15 eV photons are shown in SI (Fig. S2). The interpretation of these spectra is complicated by the contributions from bulk water ionization. The onset of liquid water ionization is around 10 eV[29,30], which means that only the first peak in the spectra can be confidently assigned to arginine alone. Moreover, we cannot exclude possible contributions from water molecules that are hydrogen bonded to arginine and from the counterions. The analysis of bulk water contributions to the spectra is given in SI. Here we focus on 12 eV spectra, because they are affected less by the bulk water ionization. By focusing on the tallest peak in the low-energy part, we observe an overall red shift of about 1 eV upon the increase of pH.

To model the photoionization spectra of solvated arginine, we carried out QM/EFP calculations following the protocols developed in our previous studies of photoionization in the condensed phase[28,31,32]. We prepared equilibrium sampling by using MD simulations and then computed VIEs of the positively charged protonated forms (p and pg) and zwitterionic forms (z, and zac) using QM/EFP. In contrast to QM/MM with non-polarizable force-fields, EFP describes electrostatic solvent effects including long-range polarization contributions calculated self-consistently[21,22]. Including polarization strongly stabilizes the ionized states, causing shifts in VIEs of up to 2 eV (see Table S3 and Fig. S8). The details of the simulations as well as the results of the benchmark study are given in the SI.

Despite the success of our computational protocol in calculating the spectra of different solvated species[28,31,32], the results for arginine are somewhat puzzling. The main challenge here is how to disentangle the contributions from water ionization from arginine ionization; this is discussed in detail in the SI. In brief, the onset of bulk water ionization is at 10 eV. Moreover, the IEs of water molecules near the carboxylate groups of arginine or around negatively charged counterions are likely to be red-shifted even further, thus affecting the low-energy spectral range. Although the calculations clearly illustrate the entanglement between ionized states of arginine and the surrounding water (i.e., as illustrated by the delocalized Dyson orbitals), there is no obvious solution of how to rigorously handle these effects. This essential feature of the valence-band photoionization limits the scope of the questions that can be addressed by these techniques. In contrast, core-level X-ray photoelectron spectroscopy can provide insight on the electronic structure of arginine[15], when electrons are ejected from C and N orbitals. But it was difficult to disentangle the contributions to the

O spectra due to the overlap with water bands, similar to what we observed here in the the valence region.

The computed spectra for the p and z forms are shown in Fig. 4b. For every form, we calculated nine lowest VIEs in each of 100 snapshots. To remove water contributions, we set a cutoff of 9.5 eV and only included the VIEs below this energy in the computed spectra (see detailed discussion in the SI). On the basis of previous studies[15], we expect the z-form to be dominant at pH 13 and the p-form to be dominant at lower pH. The comparison of the tallest peaks of these two forms in the theoretical and experimental spectra support this. We observe a theoretical red shift of 1 eV between z and p, whereas the experimental spectra show a shift of $\sim$0.3 eV for the pH 9 solution, which increases up to $\sim$1 eV in more acidic environments. However, the agreement between theory and experiment is not perfect and is, at best, semiquantitative. The main lesson learned from these calculations is that theoretical modeling and interpretation of experimental spectra of solvated species becomes complicated when water and solute ionization bands overlap. This has implication both for the design of new experiments and for the development of theoretical approaches.

In conclusion, our initial objective was to investigate the energetics of various protonation states of gas-phase arginine using valence ionization spectroscopy together with *ab initio* calculations. However, rapid and extensive fragmentation of arginine in the VUV mass spectrometer was observed. Geometry optimization and AIMD calculations show that arginine undergoes extensive fragmentation upon ionization in the gas phase. The simulations explain the low yield of parent ions and allow us to attribute the experimental photoionization onset at 8.05$\pm$0.1 eV to the ionization of the canonical isomer. The inclusion of an implicit solvent is sufficient to keep the ionized structures stable. Given the importance of solvation in stabilizing the ionized arginine, we then used valence ionization spectroscopy of solvated arginine and carried out *ab initio* calculations of the spectra. Depending on the acidity of the solvent, the population of isomers changes, and this is clearly reflected by the spectra obtained at various pHs. We expect that the p conformer is prevalent near physiological conditions, whereas the z form becomes dominant in basic solutions. The experimental spectra show an overall red shift as the pH increases. Unfortunately, the interpretation of the spectra and the comparison between the experimental and theoretical results is difficult due to the spectral overlap of valence ionization of water and arginine. Yet, the calculations show the red shift between z and p isomers, in a qualitative agreement with the experiment.

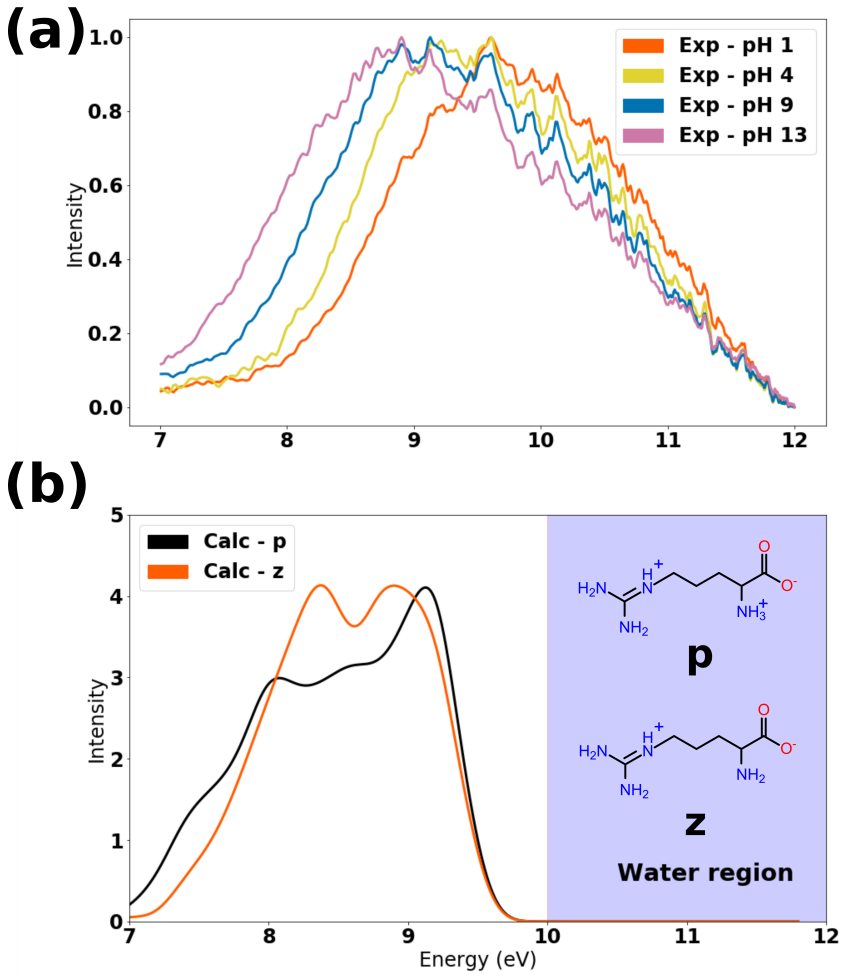

FIG. 4: (a) Experimental photoelectron spectra of aqueous arginine aerosols at various pHs measured at photon energy of 12 eV. (b) Computed spectra of protonated and zwitter-ionic forms of arginine. Only VIEs under 9.5 eV were considered for these spectra.

The inherent difficulties in disentangling the overlapping bands of solute and solvent ionization suggest that, perhaps, core-ionization techniques would help to better understand this challenging system.

Acknowledgments

This work is supported by the Department of Energy through the DE-FG02-05ER15685 grant (A.I.K.). A.I.K. is also a grateful recipient of the Simons Foundation Fellowship in Theoretical Physics. The experimental work at Berkeley lab is supported by the Director, Office of Science, Office of Basic Energy Sciences, of the U.S. Department of Energy under Contract No. DE-AC02-05CH11231, through the Condensed Phase, Interfaces and Molecular Sciences (CPIMS) program of the Chemical Sciences Division. The ALS is supported through the same contract.

The authors declare the following competing financial interest(s): A.I.K. is a member of the Board of Directors and a part-owner of Q-Chem, Inc.

Supporting Information Available: Full details of experimental and computational protocols; arginine fragments appearance energies; condensed-phase spectra obtained with 12 and 15 eV photons; comparison with the bulk water photoionization spectrum; structures, stick spectra, and Dyson orbitals of various forms of arginine; analysis of hydrogen-bonded patterns in the equilibrium MD simulations; benchmark calculations of VIEs of solvated arginine; Dyson orbitals; computed spectra of various forms of solvated arginine. This information is available free of charge via the Internet at http://pubs.acs.org.

[1] Tombola, F.; Pathak, M. M.; Isacoff, E. Y. How does voltage open an ion channel? *Annu. Rev. Cell Dev. Biol.* **2006**, *22*, 23–52.

[2] Li, L.; Vorobyov, I.; Allen, T. W. The different interactions of lysine and arginine side chains with lipid membranes *J. Phys. Chem. B* **2013**, *117*, 11906–11920.

[3] Kellermeier, M.; Rosenberg, R.; Moise, A.; Anders, U.; Przybylski, M.; Cölfen, H. Amino acids form prenucleation clusters: ESI-MS as a fast detection method in comparison to analytical ultracentrifugation *Faraday Discuss.* **2012**, *159*, 23–45.

[4] Yoshimura, Y.; Oktaviani, N. A.; Yonezawa, K.; Kamikubo, H.; Mulder, F. A. A. Unambiguous determination of protein arginine ionization states in solution by NMR spectroscopy *Angew. Chem. Int. Ed.* **2017**, *56*, 239–242.

[5] Chapo, C.J.; Paul, J.B.; Provencal, R.A.; Roth, K.; Saykally, R.J. Is arginine zwitterionic or neutral in the gas phase? Results from IR cavity ringdown spectroscopy *J. Am. Chem. Soc.* **1998**, *120*, 12956–12957.

[6] Maksic, Z.B.; Kovacevic, B. Neutral vs zwitterionic form of arginine – an ab initio study *J. Chem. Soc., Perkin Trans. 2* **1999**, *11*, 2623–2629.

[7] Wyttenbach, T.; Witt, M.; Bowers, M.T. On the stability of amino acid zwitterions in the gas phase: The influence of derivatization, proton affinity, and alkali ion addition *J. Am. Chem. Soc.* **2000**, *122*, 3458–3464.

[8] Rak, J.; Skurski, P.; Simons, J.; Gutowski, M. Low-energy tautomers and conformers of neutral and protonated arginine *J. Am. Chem. Soc.* **2001**, *123*, 11695–11707.

[9] Skurski, P.; Gutowski, M.; Barrios, R.; Simons, J. Non-ionic and zwitterionic forms of neutral arginine – an ab initio study *Chem. Phys. Lett.* **2001**, *337*, 143–150.

[10] Julian, R.R.; Jarrold, F. Gas-phase zwitterions in the absence of a net charge *J. Phys. Chem. A* **2004**, *108*, 10861–10864.

[11] Ling, S.; Yu, W.; Huang, Z.; Lin, Z.; Haranczyk, M.; Gutowski, M. Gaseous arginine conformers and their unique intramolecular interactions *J. Phys. Chem. A* **2006**, *110*, 12282–12291.

[12] Schlund, S.; Mueller, R.; Grassmann, C.; Engels, B. Conformational analysis of arginine in gas phase – a strategy for scanning the potential energy surface efficiently *J. Comput. Chem.* **2008**, *29*, 407–415.

[13] Zheng, Y.-J.; Ornstein, R.L What happens to salt-bridges in nonaqueous environments: Insights from quantum mechanics calculations *J. Am. Chem. Soc.* **1996**, *118*, 11237–11243.

[14] Julian, R.R.; Beauchamp, J.L.; Goddard III, W.A. Cooperative salt bridge stabilization of gas-phase zwitterions in neutral arginine clusters *J. Phys. Chem. A* **2002**, *106*, 32–34.

[15] Xu, B.; Jacobs, M.I.; Kostko, O.; Ahmed, M. Guanidinium group is protonated in a strongly basic arginine solution *ChemPhysChem* **2017**, *18*, 1503–1506.

[16] Shu, J.; Wilson, K. R.; Ahmed, M.; Leone, S. R. Coupling a versatile aerosol apparatus to a synchrotron: Vacuum ultraviolet light scattering, photoelectron imaging, and fragment free mass spectrometry *Rev. Sci. Instrum.* **2006**, *77*, 043106.

[17] Wilson, K.R.; Belau, L.; Nicolas, C.; Jimenez-Cruz, M.; Leone, S.R.; Ahmed, M. Direct determination of the ionization energy of histidine with VUV synchrotron radiation *Int. J. Mass Spectrom.* **2006**, *249-250*, 155–161.

[18] Kostko, O.; Xu, B.; Jacobs, M. I.; Ahmed, M. Soft X-ray spectroscopy of nanoparticles by velocity map imaging *J. Chem. Phys.* **2017**, *147*, 013931.

[19] Stanton, J. F.; Gauss, J. Analytic energy derivatives for ionized states described by the equation-of-motion coupled cluster method *J. Chem. Phys.* **1994**, *101*, 8938–8944.

[20] Krylov, A. I. Equation-of-motion coupled-cluster methods for open-shell and electronically excited species: The hitchhiker's guide to Fock space *Annu. Rev. Phys. Chem.* **2008**, *59*, 433–462.

[21] Slipchenko, L.V. Solvation of the excited states of chromophores in polarizable environment: Orbital relaxation versus polarization *J. Phys. Chem. A* **2010**, *114*, 8824–8830.

[22] Gordon, M.S.; Slipchenko, L.; Li, H.; Jensen, J.H. In *Annu. Rep. Comp. Chem.*; Spellmeyer, D.C., Wheeler, R., Eds., Vol. 3; Elsevier, 2007; p. 177.

[23] Shao, Y.; Gan, Z.; Epifanovsky, E.; Gilbert, A.T.B.; Wormit, M.; Kussmann, J.; Lange, A.W.; Behn, A.; Deng, J.; Feng, X., et al. Advances in molecular quantum chemistry contained in the Q-Chem 4 program package *Mol. Phys.* **2015**, *113*, 184–215.

[24] Hess, B.; Kutzner, C.; van derSpoel, D.; Lindahl, E. GROMACS 4: Algorithms for highly efficient, load-balanced, and scalable molecular simulation *J. Chem. Theory Comput.* **2008**, *4*, 435–447.

[25] Oana, C. M.; Krylov, A. I. Dyson orbitals for ionization from the ground and electronically excited states within equation-of-motion coupled-cluster formalism: Theory, implementation, and examples *J. Chem. Phys.* **2007**, *127*, 234106–14.

[26] Wilson, K.R.; Peterka, D.S.; Jimenez-Cruz, M.; Leone, S.R.; Ahmed, Musahid VUV photoelectron imaging of biological nanoparticles: Ionization energy determination of nanophase glycine and phenylalanine-glycine- glycine *Phys. Chem. Chem. Phys.* **2006**, *8*, 1884–1890.

[27] Ottosson, N.; Børve, K.J.; Spångberg, D.; Bergersen, H.; Saethre, L.J.; Faubel, M.; Pokapanich, W.; Öhrwall, G.; Björneholm, O.; Winter, B. On the origins of core-electron chemical shifts of small biomolecules in aqueous solution: Insights from photoemission and ab initio calculations of glycine$_{aq}$ *J. Am. Chem. Soc.* **2011**, *133*, 3120–31390.

[28] Sadybekov, A.; Krylov, A. I. Coupled-cluster based approach for core-ionized and core-excited states in condensed phase: Theory and application to different protonated forms of aqueous glycine *J. Chem. Phys.* **2017**, *147*, 014107.

[29] Winter, B.; Weber, R.; Widdra, W.; Dittmar, M.; Faubel, M.; Hertel, I.V. Full valence band photoemission from liquid water using EUV synchrotron radiation *J. Phys. Chem. A* **2004**, *108*, 2625–2632.

[30] Winter, B.; Faubel, M. Photoemission from liquid aqueous solutions *Chem. Rev.* **2006**, *106*, 1176.

[31] Ghosh, D.; Isayev, O.; Slipchenko, L. V.; Krylov, A. I. The effect of solvation on vertical ionization energy of thymine: From microhydration to bulk *J. Phys. Chem. A* **2011**, *115*, 6028–6038.

[32] Ghosh, D.; Roy, A.; Seidel, R.; Winter, B.; Bradforth, S. E.; Krylov, A. I. A first-principle protocol for calculating ionization energies and redox potentials of solvated molecules and ions: Theory and application to aqueous phenol and phenolate *J. Phys. Chem. B* **2012**, *116*, 7269–7280.

TOC graphics